DOI: 10.1002/ejic.200800330

Slow Magnetic Relaxation in $Co^{II}Cu^{II}$ Coordination Oligomer Built into Mesoporous Material

Danielle Cangussu,[a] Wallace C. Nunes,[b] Cynthia L. M. Pereira,[c] Emerson F. Pedroso,[d] Italo O. Mazali,*[a] Marcelo Knobel,[b] Oswaldo L. Alves,[a] and Humberto O. Stumpf*[e]

Keywords: Cobalt / Copper / Magnetic properties / Mesoporous materials / Molecule-based magnets

The ferrimagnetic system CoCu(opba) [opba = *ortho*-phenylenebis(oxamato)] was employed to prepare a traditional chain [CoCu(opba)]·$4H_2O$ (**1**) and a nanocomposite by incorporation in porous Vycor glass (PVG). This nanocomposite was made by first anchoring $[Bu_4N]_2$[Cu(opba)] on PVG [PVG-Cu (**2**)] and then treating it "in situ" with cobalt(II) acetate to obtain the nanomagnet PVG-CuCo (**3**). Magnetic measurements show that **1** consists of a one-dimensional ferrimagnet with strong intrachain antiferromagnetic coupling and weak interchain interactions that result in spin-glass behavior below 3.5 K. Nanocomposite **3** presents ferrimagnetic chains limited by the nanopore size, which leads to a slow relaxation of the magnetization following Arrhenius' law, frequency dependence for in-phase and out-of-phase susceptibility, and hysteresis below the blocked regime temperature (< 6 K). These features are characteristics of single-chain magnets (SCM).

Introduction

The products of molecular magnetism have a great potential to occupy an important place in science and engineering in the future. There have already been signs of this huge potential, through the synthesis of several systems with interesting properties. Spontaneous magnetization was obtained in organometallic[1] and purely organic[2] compounds. On the other hand, coordination chemistry has furnished the majority of the molecule-based magnets. The magnetic properties of these compounds have shown a great versatility: compounds exhibiting high critical temperature of magnetic ordering (T_c),[3] three types of spins and interlocked systems,[4] high coercive fields,[5] magnetic pole reversal,[6] metamagnetism,[7] conductivity,[8] photoinduced magnetization,[9] and spin transition,[10] among others, have been reported.[11]

The discovery of magnetic bistability in a dodecanuclear mixed-valence oxidomanganese(III,IV) complex, referred to as Mn_{12}, as a consequence of slow magnetic relaxation effects has opened the possibility of storing information at the single-molecule level.[12] This compound behaves as a single-molecule magnet (SMM) with a low blocking temperature (T_B) of 4.0 K.[13] More recently, slow relaxation effects, as predicted by Glauber,[14] have been found in molecular chain compounds with a strong Ising-like anisotropy of the magnetic centers and a negligible ratio of intrachain interactions. This new class of compounds has been labeled as single-chain magnets (SCMs), in analogy to SMMs.[15] Some of the reported examples of SCMs are the compounds $[Co(hfacac)_2(NITPhOMe)]$ (hfacac = hexafluoroacetylacetonate, NITPhOMe = 4′-methoxyphenyl-4,4,5,5-tetramethylimidazoline-1-oxyl-3-oxide), consisting of cobalt(II) ions and nitronyl nitroxide radicals arranged in a trigonal helix,[16] and $[CoCu(2,4,6\text{-tmpma})_2(H_2O)_2]\cdot 4H_2O$ (2,4,6-tmpma = *N*-2,4,6-trimethylphenyloxamato), an oxamato-bridged heterodimetallic chain compound.[17]

In the bottom-up strategy to build up a suitable material, the first step is the organization of a few molecules. For instance, by using the ability of porous materials, one could make ideal nanostructured systems. In recent years, a variety of materials such as multilayered Langmuir–Blodgett films,[18] silicon surfaces,[17,19] gold films,[20] and polymers[21] have been tested as host systems for the organization of SMMs. There are a few reports that use mesoporous silica materials as hosts for the incorporation of magnetic molecules. In recent studies, the acetate and benzoate derivatives of Mn_{12} have been incorporated within different types of

[a] Instituto de Química, UNICAMP,
Campinas, 13084-971, Brazil
Fax: +55-19-3521-3023
E-mail: mazali@iqm.unicamp.br
[b] Instituto de Física Gleb Wataghin, UNICAMP,
Campinas, 13084-971, Brazil
[c] Departamento de Química, UFJF,
Juiz de Fora, 36036-330, Brazil
[d] Departamento de Química, CEFET-MG,
Belo Horizonte, 30480-000, Brazil
[e] Departamento de Química, ICEx, Universidade Federal de Minas Gerais,
Av. Antônio Carlos, 6627, Pampulha, Belo Horizonte, MG, 31270-901, Brazil
Fax: +55-31-34095700
E-mail: stumpf@dedalus.lcc.ufmg.br

Supporting information for this article is available on the WWW under http://www.eurjic.org or from the author.

mesoporous silica.[22–26] The magnetic properties of these nanocomposite materials are practically identical to the crystalline phase, indicating that the structures of the cluster are the same after incorporation. In addition, mesoporous silica materials have been employed as the host support for an octanuclear oxamatonickel(II) complex of formula $\{[Ni_2(mpba)_3][Ni(dpt)(H_2O)]_6\}(ClO_4)_4 \cdot 12.5H_2O$ [mpba = *N,N′*-1,3-phenylenebis(oxamato), dpt = dipropylenetriamine] showing a moderately anisotropic $S = 4$ ground spin state that behaves as a SMM at low temperatures ($T_B = 3.0$ K).[25] In this case, the nanocomposite materials showed an exotic spin-glass magnetic behavior.

Our group has studied magnetic systems that are candidates to present SCM behavior, such as [CoCu(opba)(dmso)$_3$],[27] where opba is *ortho*-phenylenebis(oxamato).[28] This ferrimagnet chain, in spite of the presence of anisotropy, strong intrachain coupling, and good interchain isolation, did not show much promise. In addition, the reports on *infinite* chains that follow the predicted Glauber dynamics are presented as magnetically segmented.[16,17] Therefore, we decided to confine the CoCu(opba) system to see whether the magnetic properties run in this direction. Our choice for confinement was porous Vycor glass (PVG), which has an open porous structure of fundamentally pure silica with interconnecting pores ranging from 2 to 20 nm.[29] In this glass, the volume of pores represents approximately 28% of the total volume, and the average pore diameter is 4 nm.[30] The porous surface contains silanol groups, with acidic hydrogen atoms ($pK_a \approx 9$), which can be used as active sites for the incorporation of several compounds. In fact, this glass has been successfully used to produce nanocomposites of a great variety of compounds such as complexes, semiconductors, oxides, and polymers.[31–34] Otherwise, the porous materials employed for the incorporation of magnetic molecules are the functionalized and nonfunctionalized SBA-15[26] or MCM-41-type ordered mesoporous silica with pore sizes ranging from 2 to 15 nm. These materials are mesostructured with channels in highly ordered two-dimensional hexagonal arrays. Both PVG and ordered mesoporous silica are noncrystalline materials with a high density of silanol groups on the porous surface. PVG exhibits a large and random distribution of pore sizes in comparison with SBA-15 or MCM-41.

In this paper, we report on the synthesis of the coordination polymer $\{[CoCu(opba)] \cdot 4H_2O\}_n$ (**1**) and the first immobilization of oligomers of this type of 1D system onto mesoporous reactors (PVG) by using a new synthetic route. The nanocomposite was prepared in two separate steps. In the first, the building block $[Cu(opba)]^{2-}$ (Scheme 1)[28] was incorporated into PVG (PVG-Cu, **2**). In the second step, as for the synthesis of **1**, the $[Cu(opba)]^{2-}$ behaves as a bis(bidentate) ligand for coordination to the cobalt(II) ions, now in the inorganic host matrix, leading to the nanocomposite PVG-CuCo (**3**).

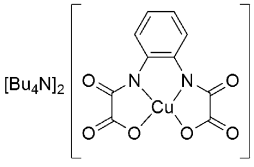

Scheme 1. Structural formula of the $[Bu_4N]_2[Cu(opba)]$ complex.

Results and Discussion

Synthesis and General Physical Characterization

Attempts to obtain single crystals of **1** were not successful; the compound was characterized by elemental analysis, IR spectroscopy, X-ray powder diffraction (see Supporting Information), and magnetochemistry studies. The quantity of solvent molecules was confirmed by thermogravimetric and differential thermal analysis. The IR spectrum of **1** presents an important number of peaks due to the presence of the opba ligand. Among them, two intense bands appear at 1602 and 1576 cm^{-1}, which are attributed to the C=O stretching vibration.[35]

As for the nanoporous confinement, at the first step, the impregnation of $[Bu_4N]_2[Cu(opba)]$ precursor leads to nanocomposite **2**. In order to investigate the host–guest mechanism, diffuse reflectance infrared (DR-IR) spectra were collected from PVG plates before and after the impregnation process. The spectra obtained from PVG are presented in Figure 1. The PVG DR-IR spectrum shows a sharp band located at 3745 cm^{-1} attributed to the free O–H stretching mode of surface silanols (Figure 1a). This band disappears after impregnation of the precursor to form **2** (Figure 1b). In addition, intense bands located at 2966, 2942, and 2979 cm^{-1}, attributed to C–H stretching of NBu_4^+ and the opba ligand, clearly indicate that the precursor molecules were impregnated into the porous Vycor glass. The PVG porous surface presents silanol groups, which makes this material an ion-exchanger. Cationic species such as NBu_4^+ displace the slightly acidic ($pK_a \approx 9$) silanol protons. Furthermore, $[Cu(opba)]^{2-}$ is a weak base capable of accepting one or two protons to form an iminoalcohol compound.

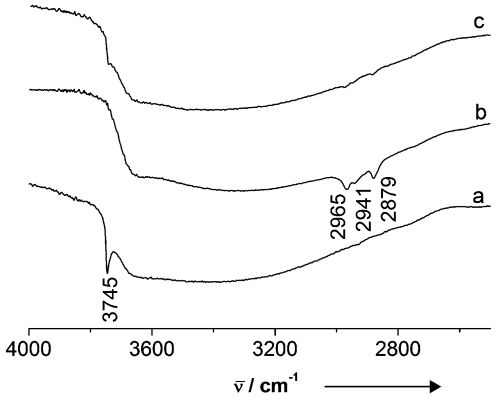

Figure 1. DR-IR spectra of (a) PVG, (b) **2**, and (c) **3**.

The preparation of nanocomposite **3**, in the second reaction, is shown by a color change from deep-purple (the characteristic color of $[Bu_4N]_2[Cu(opba)]$) to blue (the characteristic color of [CoCu(opba)]). When cobalt acetate is added to **2**, Co^{II} ions are absorbed by an ion-exchange reaction and coordination to the $[Cu(opba)]^{2-}$ to yield a chain of $[CoCu(opba)]_n$ inside the PVG pores; species such as NBu_4^+ and CH_3COO^- are left in solution. The DR-IR spectrum of **3** (Figure 1c) shows that the bands attributed to NBu_4^+ undergo a loss in intensity after the second reaction inside the pores.

The chemical identities of the adsorbed species were investigated by Raman spectroscopy with spatial resolution (Figure 2) on the cutting side of a blade. The Raman spectra of plates **2** (Figure 2a) and **3** (Figure 2b) below 500 cm^{-1} are nearly free from the interference of the spectroscopic features of the glass, presenting the same bands as observed for the spectra obtained for the free compounds. These Raman spectroscopic data also indicate that the bands located in the 2850–3000 cm^{-1} region, characteristic of the C–H stretching of NBu_4^+, fully disappear in the spectrum of **3**. The most intense band present in the spectrum of **2** occurs at 1401 cm^{-1} and is assigned to the symmetric ν_{COO} vibrations of monodentate carboxylato groups. This band is shifted toward 1421 cm^{-1} for **3**. This shift agrees with what is expected for the symmetric ν_{COO} vibration for bridging carboxylato groups, confirming cobalt coordination to the $[Cu(opba)]^{2-}$ terminal oxygen atoms in **3**.

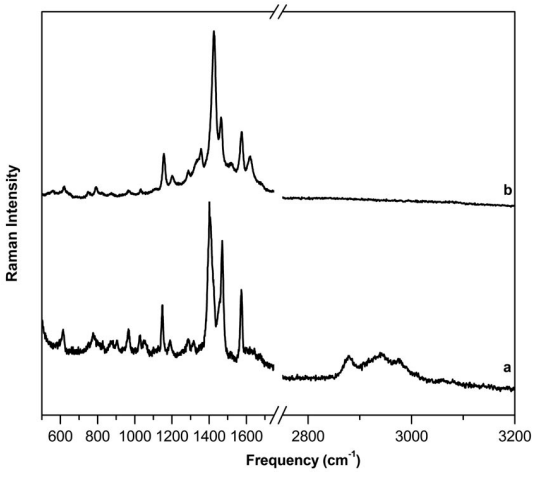

Figure 2. Raman spectra of (a) **2** and (b) **3**.

The specific surface area (SSA) data obtained by nitrogen adsorption confirm that the chain grew inside the pores of PVG, as the pristine PVG had a SSA about 250 m^2g^{-1}, whereas the SSA decreased to 110 m^2g^{-1} after the procedure for the synthesis of **3** was carried out.

X-ray mapping (see Supporting Information) and transmission electron microscopy (TEM) images obtained from nanocomposite **3** reveal the presence of $[CoCu(opba)]_n$ in the sample. TEM bright-field images, shown in Figure 3, reveal the presence of CoCu nanocrystals as dark spots homogeneously dispersed in the PVG matrix. Initially, we observed a low contrast between $\{[CoCu(opba)]\}_n$ and the glass (Figure 3a, with a mean nanocrystal size of about 3.2 nm). However, after some minutes, a new image resulted (Figure 3b) from the interaction of **3** with the electron beam, and it became clear that the material contained very small nanoparticles with a rather narrow size dispersion (see inset in Figure 3b), having a mean nanocrystal size of about 5.2 nm.

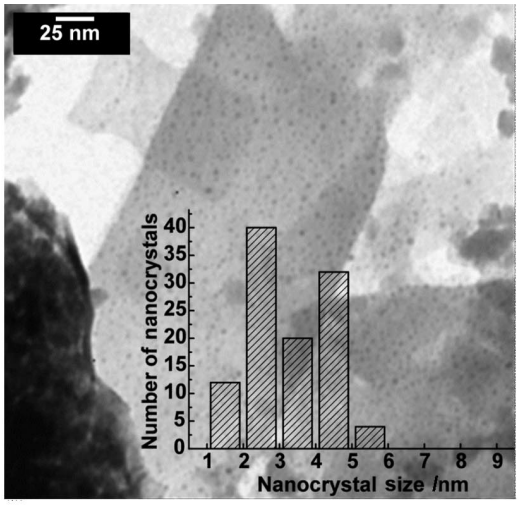

(a)

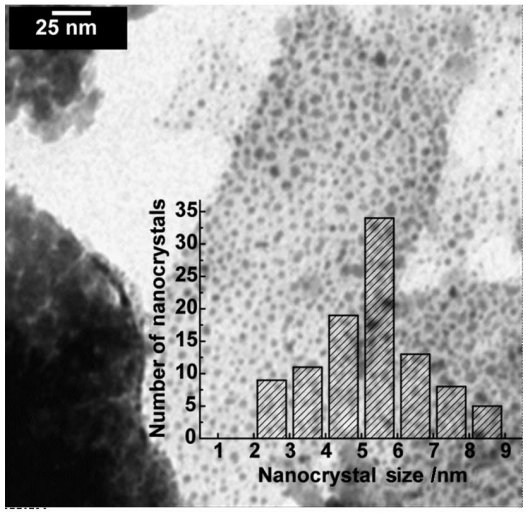

(b)

Figure 3. TEM bright-field image for **3** (a) with the lowest time for interaction with the beam and (b) after some minutes of interaction with the beam. The insets show the particle-size distribution.

Magnetic Properties

The magnetic susceptibility data of **1** are shown in Figure 4 in the form of a $\chi_M T$ versus T plot, χ_M being the magnetic susceptibility and T the temperature. The data were measured with an applied field of 50 Oe throughout the whole temperature range. As the temperature is lowered, $\chi_M T$ decreases smoothly and then reaches a round minimum at 85 K. It then increases as T is lowered further. A

minimum in the $\chi_M T$ versus T plot in compounds having $[CoCu(opba)]_n$ has been observed by several authors[27,36] and associated to one-dimensional ferrimagnetic behavior as a consequence of antiferromagnetic coupling between the magnetic moments of Co^{II} and Cu^{II}. At the temperature where the minimum of $\chi_M T$ occurs, the coupling is short-range, but the correlation length increases as the temperature is further lowered as a result of the reduction of randomizing thermal effects. In this case, the Co^{II} magnetic moments tend to align along the applied field direction, while the Cu^{II} magnetic moments align along the opposite one. In addition, there is no maximum in the χ_M versus T plot of **1** (data not shown), which indicates the absence of long-range antiferromagnetic order in this compound. The observed maximum in the $\chi_M T$ versus T plot is indeed due to saturation effects.

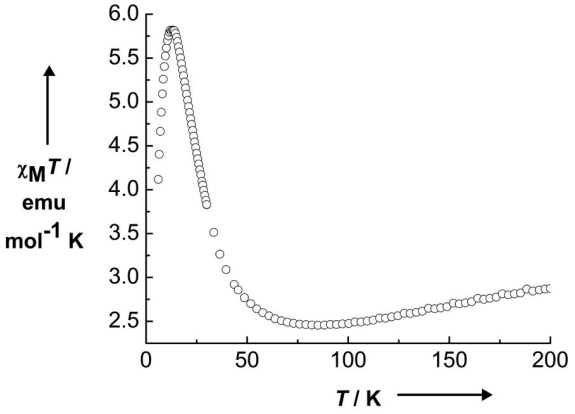

Figure 4. $\chi_M T$ versus T plot for **1** at an applied field (H) of 50 Oe.

In order to obtain further information on the low-temperature magnetic ordering of **1**, the dynamics of the magnetization was studied by measuring the thermal dependence of both in-phase (χ') and out-of-phase (χ'') components of the ac susceptibility for different frequencies of the alternating ac field, ω. Figure 5 shows the temperature dependence of χ' and χ'' obtained for **1**. The nonzero value observed for χ'' in the low-temperature range indicates a three-dimensional magnetic ordering or a blocking process. Both components of the susceptibility display a maximum at almost the same temperature, and the variation of the maxima with the frequency is very small.

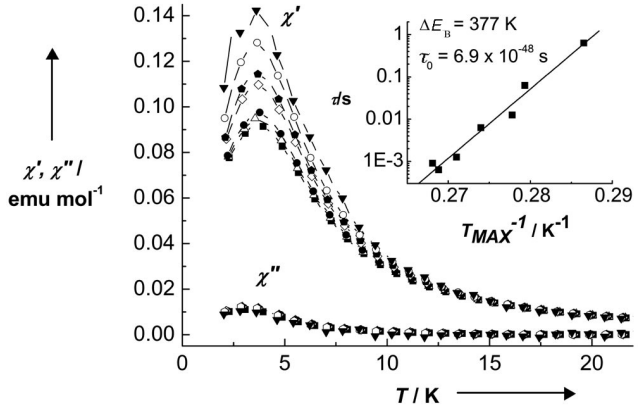

Figure 5. Thermal dependence of in-phase (χ') and out-of-phase (χ'') ac magnetic susceptibility measured at (■) 10 kHz, (Δ) 7 kHz, (●) 5 kHz, (✧) 1 kHz, (filled pentagon) 500 Hz, (○) 100 Hz, and (▾) 10 Hz, under a zero dc field and an ac field of 4 Oe for **1**. The inset shows the log (τ) vs $1/T_{MAX}$ plot for all measured frequencies.

Relaxation by a thermal activation mechanism follows the well-known Arrhenius' law,

$$\tau = \tau_0 \exp\left(\frac{\Delta E}{k_B T}\right)$$

where ΔE is the activation energy, k_B the Boltzmann constant, and τ_0 the characteristic time constant, usually taken in the 10^{-11}–10^{-9} s range. The relaxation time of the ordering observed for **1** can be extracted from the maximum of the χ'' component, because, at this temperature, $\tau^{-1}(T_{MAX}) = \bar{\omega}$. The results are shown in the inset of Figure 5. The relaxation of **1** follows Arrhenius' law rather well, and the best linear fit leads to $\tau_0 = 6.9 \times 10^{-48}$ s and $\Delta E/k_B = 377$ K. The unphysical small value of the characteristic time τ_0 obtained from this analysis is an indication of a spin-glass-like behavior, as has been suggested by other authors.[37] A quantitative measurement of the relative variation of T_{MAX} per decade of frequency, $(\Delta T_{MAX}/T)/\Delta\log(\bar{\omega})$, gives the value 0.022, which is in the range associated with spin-glass systems characterized by short-range interactions (as observed in insulating and semiconductor spin-glasses).[38] This behavior may be attributed to interchain interactions (dipolar and/or superexchange through solvent molecules) forming regions of diameter given by the magnetic correlation length, as already observed in granular magnetic systems.[39]

The chain confined in PVG presents significant differences in its magnetic properties in relation to **1** and other reported oxamato-based $Co^{II}Cu^{II}$ ferrimagnets. The χT versus T curve of **3** (see Supporting Information) is similar to that of **1**, except that the minimum is shifted to a lower temperature (around 60 K). Figure 6 shows the temperature dependence of the zero-field-cooled (M_{ZFCM}) and field-cooled (M_{FCM}) magnetization with an applied field (H_{DC}) of 20 Oe for **3**. The separation between the M_{ZFCM} and M_{FCM} curves can be due to a magnetic ordering or a slow relaxation below the irreversibility temperature of around 6 K.

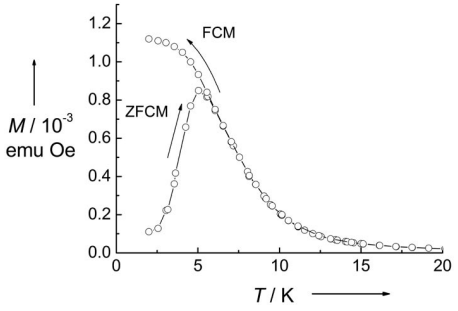

Figure 6. Zero-field-cooled (ZFCM) and field-cooled (FCM) magnetization as a function of temperature for **3**, with an applied field of 20 Oe.

The field dependence of the magnetization up to 65 kOe at different temperatures was also investigated. Figure 7 shows a magnetization loop measured at 2 K for **3**, which displays a narrow hysteresis loop with a coercive field of 780 Oe. Even at 65 kOe, the saturation magnetization was not reached. The coercive field decreases as the temperature increases, going down to zero at the irreversibility temperature (see lower-right inset of Figure 7).

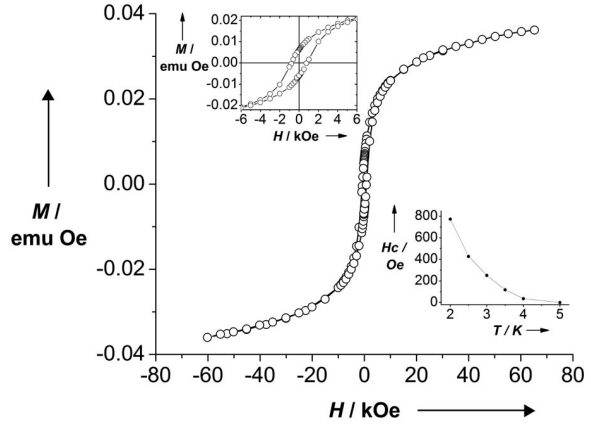

Figure 7. Hysteresis loop of **3** at 2.0 K. The upper-left inset shows details of the loop for low fields, where a coercive field of 780 Oe is observable. The lower-right inset shows the temperature dependence of the coercive field obtained from hysteresis loops measured at different temperatures.

The dynamics of the magnetization for **3** was studied by measuring the temperature dependence of both in-phase and out-of-phase components of the ac susceptibility for different frequencies of the alternating ac field. Figure 8 shows these measurements performed under a zero dc field. The components of the susceptibility of **3** display a maximum at different temperatures, depending on the measurement frequency, which confirms the slow relaxation of the magnetization (blocking) in the low-temperature regime (< 6 K).

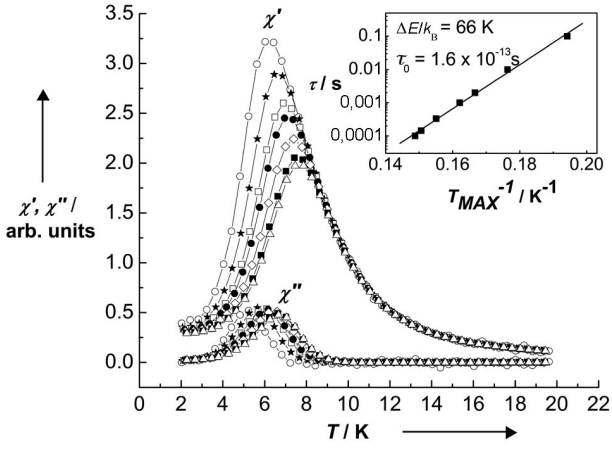

Figure 8. χ' and χ'' versus T measured at (Δ) 10 kHz, (■) 7 kHz, (✧) 3 kHz, (●) 1 kHz, (□) 500 Hz, (★) 100 Hz, and (○) 10 Hz, under a zero dc field and an ac field of 4 Oe for **3**. The inset shows the $\log(\tau)$ versus $1/T_{MAX}$ plot for all measured frequencies.

The relaxation of **3** follows Arrhenius' law, and the best linear fit leads to $\tau_0 = 1.6 \times 10^{-13}$ s and $\Delta E/k_B = 66$ K. A quantitative measurement of the relative variation of T_{MAX} per decade of frequency, $(\Delta T_{MAX}/T)/\Delta\log(\bar{\omega})$, leads to the value 0.08, which is not far from that (0.1) for the SCM $[Co(hfacac)_2(NITPhOMe)]$.[16]

Slow magnetic relaxation following Arrhenius' law has been observed in SCMs with finite segments of one dimensional (1D) chains, as predicted by Glauber for 1D Ising systems.[40] In such molecular materials, a collective reversal of short segments of molecular Ising chains (e.g. Co-PhOMe) was theoretically predicted and experimentally observed.[12a,15,39,40] Our system **3** presents short chains that are limited by the Vycor pores. As a result, it is expected that the Co^{II} ions of such oligomers experience a strong Ising anisotropy due to the low symmetry of its structural environment. Therefore, the magnetization dynamics observed for **3** should have the same mechanism as the SCM.

Conclusions

In the work presented herein, we have synthesized and characterized polymeric ferrimagnet **1** and oligomeric-confined ferrimagnet **3** CoCu(opba), presenting slow relaxation of magnetization. Compound **1** is a usual chain obtained in aqueous solution. It is a one-dimensional ferrimagnet with strong intrachain antiferromagnetic coupling as in the similar chain $[CoCu(opba)(dmso)_3]$.[27] For this latter chain, SCM characteristics are not observed in spite of the better chain isolation by large solvent molecules. Therefore, this CoCu(opba) system suggests that achievement of SCMs is a more complex task, and that the presence of anisotropy and a large ratio of intrachain to interchain coupling constants ($|J/j| > 10^4$) are not enough. The challenge is to attain a real Ising system with magnetically correlated segments in long chains. In this direction, the second part of this work brings new insights. When the chain lengths were limited by the nanopore sizes of the PVG matrix, the resulting nanocomposite **3** showed a blocking behavior below 6 K, similar to that observed in SCMs. In fact, the τ_0 value (1.6×10^{-13} s) is close to that of other SCMs, as for example the $\{[Fe^{III}\{HB(pz)(CN)_3\}_2Cu(MeOH)\}\cdot 2MeOH$ chain with $\tau_0 = 2.8 \times 10^{-13}$ s.[41] The low value observed for τ_0 in the present case, with regard to the characteristic superparamagnetic time constant (10^{-11}–10^{-9} s), indicates that the short chains interact weakly within the nanopores. This new synthetic route to control the size of molecule-based polymeric magnets by incorporation into nanoporous Vycor glass opens new perspectives for the preparation and tailoring of multiproperty magnetic materials.

Experimental Section

Materials and Methods: PVG, code 7930, was purchased from Corning Glass. It is a transparent porous material obtained by acid leaching of a phase-separated alkaline borosilicate glass. To remove impurities, a PVG plate with dimensions of

10 mm × 10 mm × 0.5 mm was first immersed in a HCl solution (2 M) for 2 h and then in acetone for the same period. After being dried, the PVG plate was heated at 823 K for 72 h and then cooled to room temperature before being stored in a desiccator. The $[Bu_4N]_2[Cu(opba)]$ and $Na_2[Cu(opba)]\cdot 3H_2O$ used in this work were synthesized by following the methods described in the literature.[28]

$[CoCu(opba)]\cdot 4H_2O$ (1): Compound **1** was prepared by adding an aqueous solution of $Co(NO_3)_2\cdot 6H_2O$ (282 mg, 0.97 mmol, 5 mL), previously dissolved in warm water (50 °C), to a solution of $Na_2[Cu(opba)]\cdot 3H_2O$ (400 mg, 0.97 mmol, 20 mL), previously dissolved in water at the same temperature. After that, a dark blue polycrystalline powder was obtained. The compound was filtered, washed with water, and dried under vacuum in a desiccator. Yield: 329 mg (77%). $C_{10}H_{12}CoCuN_2O_{10}$ (442.64): C 27.13, H 2.71, Cu 14.35, Co 13.31, N 6.33; found: C 26.66, H 2.51, Cu 14.25, Co 12.29, N 6.18. IR (KBr): $\tilde{\nu}$ = 3486, 3424 (O–H), 1602, 1576 (C=O), 1464, 1417 (C=C), 1357 (C–N), 587, 552 (Cu–O) cm^{-1}.

PVG-Cu (2): The previously cleaned PVG plate was immersed in a flask containing a dichloromethane solution of $[Bu_4N]_2[Cu(opba)]$ (25 mL, 0.01 M) for 72 h. The PVG plate became deep-purple, the same color as the $[Bu_4N]_2[Cu(opba)]$ solution. It was washed with dichloromethane to remove the excess precursor absorbed on the glass surface and dried under vacuum.

Nanocomposite PVG-CuCo (3): Plate **2** was immersed in a flask containing an aqueous solution of $Co(CH_3COO)_2\cdot 4H_2O$ (25 mL, 0.1 M) for 24 h. After this period, the plate was washed with water and dried under vacuum. Nanocomposite **3**, obtained after these two steps of impregnation, has a blue color.

Physical Techniques: The diffuse reflectance infrared (DR-IR) spectra were obtained by using crushed samples with a Nicolet 520 spectrophotometer. Raman spectra were obtained with a Renishaw Raman Imaging Microprobe System 3000 spectrometer, equipped with an optical microscope with spatial resolution. The spectral excitation was provided by a He–Ne laser, with the 632.8 nm laser line (8 mW). The slits were set for a resolution of 2 cm^{-1}. The specific surface area was obtained by N_2 adsorption/desorption isotherms (ASAP2010 analyzer). Scanning electron microscopy was performed with a JSM 6360 LV electron microscope. The images were analyzed by energy-dispersive X-ray spectrometry (EDX). Transmission electron microscopy images were obtained from a Zeiss CEM 902 microscope operating at 100 kV. A small amount of the crushed sample was first suspended in water and allowed to settle for 5 min. A drop of the supernatant dispersion was then placed onto a Parlodion film supported by a copper grid. Magnetic measurements were carried out with a superconducting quantum interference device (SQUID) magnetometer (Quantum Design MPMS XL7) in the temperature range 2–300 K. Magnetic susceptibility was measured with a Physical Properties Measuring System (Quantum Design PPMS) in the frequency range 10–10 kHz.

Supporting Information (see footnote on the first page of this article): X-ray powder diffractogram of **1**; X-ray mapping, gas sorption isotherms, and $\chi_M T$ versus T curve for **3**.

Acknowledgments

D. C. and W. C. N. acknowledge financial support (postdoc grant) from the Brazilian agencies Conselho Nacional de Desenvolvimento Científico e Tecnológico (CNPq) and Fundação de Amparo à Pesquisa do Estado de São Paulo (FAPESP). This work was partially supported by Coordenação de Aperfeiçoamento de Pessoal de Nível Superior (CAPES/COFECUB), Fundação de Amparo à Pesquisa do Estado de Minas Gerais (FAPEMIG), and Millennium Institute for Complex Materials. The authors are grateful to Prof. D. L. A. Faria and Prof. M. L. A. Temperini (IQ-USP, Brazil) for the assistance in Raman spectroscopic measurements and to Prof. C. H. Collins (IQ-UNICAMP, Brazil) for revision of the English.

[1] a) J. S. Miller, J. C. Calabrese, H. Rommelmann, S. R. Chittipeddi, J. H. Zhang, W. M. Reiff, A. J. Epstein, *J. Am. Chem. Soc.* **1987**, *109*, 769–781; b) J. M. Manriquez, G. T. Yee, R. S. Mclean, A. J. Epstein, J. S. Miller, *Science* **1991**, *252*, 1415–1417.
[2] R. Chiarelli, M. A. Novak, A. Rassat, J. L. Tholence, *Nature* **1993**, *363*, 147–149.
[3] S. Ferlay, T. Mallah, R. Ouahes, P. Veillet, M. Verdaguer, *Nature* **1995**, *378*, 701–703.
[4] a) H. O. Stumpf, L. Ouahab, Y. Pei, D. Grandjean, O. Kahn, *Science* **1993**, *261*, 447–449; b) M. G. F. Vaz, M. Knobel, N. L. Speziali, A. M. Moreira, A. F. C. Alcantara, H. O. Stumpf, *J. Braz. Chem. Soc.* **2002**, *13*, 183–189.
[5] a) H. O. Stumpf, Y. Pei, C. Michaut, O. Kahn, J. P. Renard, L. Ouahab, *Chem. Mater.* **1994**, *6*, 257–259; b) M. Kurmoo, C. J. Kepert, *New J. Chem.* **1998**, *22*, 1515–1524; c) M. C. Dias, M. Knobel, H. O. Stumpf, *J. Magn. Magn. Mater.* **2001**, *226*, 1961–1963.
[6] a) C. Mathoniere, C. J. Nuttall, S. G. Carling, P. Day, *Inorg. Chem.* **1996**, *35*, 1201–1206; b) O. Cador, M. G. F. Vaz, H. O. Stumpf, C. Mathoniere, O. Kahn, *Synth. Met.* **2001**, *122*, 559–567.
[7] a) F. Lloret, R. Ruiz, M. Julve, J. Faus, Y. Journaux, I. Castro, M. Verdaguer, *Chem. Mater.* **1992**, *4*, 1150–1153; b) C. L. M. Pereira, E. F. Pedroso, H. O. Stumpf, M. A. Novak, L. Ricard, R. Ruiz-Garcia, E. Riviere, Y. Journaux, *Angew. Chem. Int. Ed.* **2004**, *43*, 955–958.
[8] a) P. Day, M. Kurmoo, T. Mallah, I. R. Marsden, R. H. Friend, F. L. Pratt, W. Hayes, D. Chasseau, J. Gaultier, G. Bravic, L. Ducasse, *J. Am. Chem. Soc.* **1992**, *114*, 10722–10729; b) E. Coronado, J. R. Galan-Mascaros, C. J. Gomez-Garcia, V. Laukhin, *Nature* **2000**, *408*, 447–449.
[9] a) O. Sato, T. Iyoda, A. Fujishima, K. Hashimoto, *Science* **1996**, *272*, 704–705; b) D. A. Pejakovic, J. L. Manson, J. S. Miller, A. J. Epstein, *Phys. Rev. Lett.* **2000**, *85*, 1994–1997.
[10] a) O. Kahn, C. J. Martinez, *Science* **1998**, *279*, 44–48; b) J. A. Real, A. B. Gaspar, V. Niel, M. C. Munoz, *Coord. Chem. Rev.* **2003**, *236*, 121–141.
[11] J. S. Miller, M. Drillon (Eds.), *Magnetism: Molecules to Materials*, Wiley-VCH, Weinheim, **2001**.
[12] a) R. Sessoli, D. Gatteschi, A. Caneschi, M. A. Novak, *Nature* **1993**, *365*, 141–143; b) D. Gatteschi, A. Caneschi, L. Pardi, R. Sessoli, *Science* **1994**, *265*, 1054–1058.
[13] a) J. R. Friedman, M. P. Sarachik, J. Tejada, J. Maciejewski, R. Ziolo, *J. Appl. Phys.* **1996**, *79*, 6031–6033; b) L. Thomas, F. Lionti, R. Ballou, D. Gatteschi, R. Sessoli, B. Barbara, *Nature* **1996**, *383*, 145–147.
[14] R. J. Glauber, *J. Math. Phys.* **1963**, *4*, 294–307.
[15] L. Bogani, A. Caneschi, M. Fedi, D. Gatteschi, M. Massi, M. A. Novak, M. G. Pini, A. Rettori, R. Sessoli, A. Vindigni, *Phys. Rev. Lett.* **2004**, *92*, 207204.
[16] A. Caneschi, D. Gatteschi, N. Lalioti, C. Sangregorio, R. Sessoli, G. Venturi, A. Vindigni, A. Rettori, M. G. Pini, M. A. Novak, *Angew. Chem. Int. Ed.* **2001**, *40*, 1760–1763.
[17] a) E. Pardo, R. Ruiz-Garcia, F. Lloret, J. Faus, M. Julve, Y. Journaux, F. Delgado, C. RuizPerez, *Adv. Mater.* **2004**, *16*, 1597–1600; b) E. Pardo, R. Ruiz-Garcia, F. Lloret, J. Faus, M. Julve, Y. Journaux, M. Novak, F. Delgado, C. Ruiz-Perez, *Chem. Eur. J.* **2007**, *13*, 2054–2066.
[18] M. Clemente-Leon, H. Soyer, E. Coronado, C. Mingotaud, C. J. Gomez-Garcia, P. Delhaes, *Angew. Chem. Int. Ed.* **1998**, *37*, 2842–2845.

[19] M. Mannini, D. Bonacchi, L. Zobbi, F. M. Piras, E. A. Speets, A. Caneschi, A. Cornia, A. Magnani, B. J. Ravoo, D. N. Reinhoudt, R. Sessoli, D. Gatteschi, *Nano Lett.* **2005**, *5*, 1435–1438.
[20] E. Coronado, A. Forment-Aliaga, F. M. Romero, V. Corradini, R. Biagi, V. De Renzi, A. Gambardella, U. del Pennino, *Inorg. Chem.* **2005**, *44*, 7693–7695.
[21] F. Palacio, P. Oliete, U. Schubert, I. Mijatovic, N. Husing, H. Peterlik, *J. Mater. Chem.* **2004**, *14*, 1873–1878.
[22] T. Coradin, J. Larionova, A. A. Smith, G. Rogez, R. Clerac, C. Guerin, G. Blondin, R. E. P. Winpenny, C. Sanchez, T. Mallah, *Adv. Mater.* **2002**, *14*, 896–898.
[23] M. Clemente-Leon, E. Coronado, A. Forment-Aliaga, P. Amoros, J. Ramirez-Castellanos, J. M. Gonzalez-Calbet, *J. Mater. Chem.* **2003**, *13*, 3089–3095.
[24] M. Clemente-Leon, E. Coronado, A. Forment-Aliaga, J. M. Martinez-Agudo, P. Amoros, *Polyhedron* **2003**, *22*, 2395–2400.
[25] E. Pardo, P. Burguete, R. Ruiz-Garcia, M. Julve, D. Beltran, Y. Journaux, P. Amoros, F. Lloret, *J. Mater. Chem.* **2006**, *16*, 2702–2714.
[26] S. Willemin, G. Arrachart, L. Lecren, J. Larionova, T. Coradin, R. Clérac, T. Mallah, C. Guérin, C. Sanchez, *New J. Chem.* **2003**, *27*, 1533–1539.
[27] C. L. M. Pereira, A. C. Doriguetto, C. Konzen, L. C. MeiraBelo, U. A. Leitao, N. G. Fernandes, Y. P. Mascarenhas, J. Ellena, A. L. Brandl, M. Knobel, H. O. Stumpf, *Eur. J. Inorg. Chem.* **2005**, 5018–5025.
[28] O. Kahn, H. Stumpf, Y. Pei, J. Sletten, *Mol. Cryst. Liq. Cryst.* **1993**, *233*, 231–246.
[29] M. O. Adebajo, H. D. Gesser, *Appl. Surf. Sci.* **2001**, *171*, 120–124.
[30] M. B. Volf, *Technical Approach to Glass*, Elsevier, Amsterdam, **1990**.
[31] a) I. F. Gimenez, O. L. Alves, *J. Braz. Chem. Soc.* **2004**, *15*, 640–645; b) D. J. Maia, A. J. G. Zarbin, O. L. Alves, M. A. De Paoli, *Adv. Mater.* **1995**, *7*, 792–796.
[32] I. O. Mazali, R. Romano, O. L. Alves, *Thin Solid Films* **2006**, *495*, 64–67.
[33] I. O. Mazali, A. G. Souza Filho, B. C. Viana, J. Mendes Filho, O. L. Alves, *J. Nanoparticle Res.* **2006**, *8*, 141–148.
[34] P. T. Sotomaior, I. M. Raimundo Jr, A. J. G. Zarbin, J. J. R. Rohwedder, G. Oliveira Neto, O. L. Alves, *Sens. Actuators B* **2001**, *74*, 157–162.
[35] K. Nakamoto, *Infrared and Raman Spectra of Inorganic and Coordination Compounds*, 4th ed., Wiley, New York, **1986**.
[36] J. Larionova, S. A. Chavan, J. V. Yakhmi, A. G. Froystein, J. Sletten, C. Sourisseau, O. Kahn, *Inorg. Chem.* **1997**, *36*, 6374–6381.
[37] J. A. Mydosh, *Spin Glass: An Experimental Introduction*, Taylor and Francis, London, **1993**.
[38] a) J. L. Dormann, D. Fiorani, E. Tronc, *J. Magn. Magn. Mater.* **1999**, *202*, 251–267; b) C. L. M. Pereira, E. F. Pedroso, M. A. Novak, A. L. Brandl, M. Knobel, H. O. Stumpf, *Polyhedron* **2003**, *22*, 2387–2390.
[39] W. C. Nunes, L. M. Socolovsky, J. C. Denardin, F. Cebollada, A. L. Brandl, M. Knobel, *Phys. Rev. B* **2005**, *72*, 212413-1–212413-4.
[40] A. Vindigni, A. Rettori, L. Bogani, A. Caneschi, D. Gatteschi, R. Sessoli, M. A. Novak, *Appl. Phys. Lett.* **2005**, *87*, 73102-1–73102-3.
[41] S. Wang, J. L. Zuo, S. Gao, Y. Song, H. C. Zhou, Y. Z. Zhang, X. Z. You, *J. Am. Chem. Soc.* **2004**, *126*, 8900–8901.

Received: March 31, 2008
Published Online: July 9, 2008

